

Article

Pseudoflow with OCT Angiography in Eyes with Hard Exudates and Macular Drusen

Kirk K. Hou¹, Adrian Au¹, Amir H. Kashani², K. Bailey Freund^{3,4}, Srinivas R. Sadda^{1,5}, and David Sarraf^{1,6,7}

¹ Department of Ophthalmology, David Geffen School of Medicine, University of California Los Angeles, Los Angeles, CA, USA

² Department of Ophthalmology, USC Roski Eye Institute, Keck School of Medicine, University of Southern California, Los Angeles, CA, USA

³ Vitreous Retina Macula Consultants of New York, New York, NY, USA

⁴ Department of Ophthalmology, New York University School of Medicine, New York, NY, USA

⁵ Doheny Image Reading Center, Doheny Eye Institute, Los Angeles, CA, USA

⁶ Retinal Disorders and Ophthalmic Genetics Division, Stein Eye Institute, David Geffen School of Medicine, University of California Los Angeles, Los Angeles, CA, USA

⁷ Greater Los Angeles VA Healthcare Center, Los Angeles, CA, USA

Correspondence: David Sarraf, Retinal Disorders and Ophthalmic Genetics Division, Stein Eye Institute, David Geffen School of Medicine at UCLA, 100 Stein Plaza, Los Angeles, CA, USA. e-mail: dsarraf@ucla.edu

Received: 18 December 2018

Accepted: 21 April 2019

Published: 27 June 2019

Keywords: RVO; macular edema; age-related macular degeneration; OCTA; artifact

Citation: Hou KK, Au A, Kashani AH, Freund KB, Sadda SR, Sarraf D. Pseudoflow with OCT angiography in eyes with hard exudates and macular drusen. *Trans Vis Sci Tech.* 2019;8(3):50, <https://doi.org/10.1167/tvst.8.3.50>
Copyright 2019 The Authors

Purpose: To analyze “pseudoflow,” a false positive flow-artifact observed with optical coherence tomography angiography (OCTA) of stationary hyperreflective structures corresponding to hard exudates and macular drusen.

Methods: Retrospective case series of patients with hard exudates (due to diabetic macular edema [DME] or retinal vein occlusion [RVO]) or macular drusen (due to nonneovascular, or dry, age-related macular degeneration [AMD]) studied with OCTA by using volume-based projection artifact removal (3D PAR).

Results: OCTA of 20 eyes (10 DME/10 RVO) with hard exudates were analyzed. All eyes exhibited pseudoflow corresponding to hard exudates. Seven eyes concurrently demonstrated hard exudates without pseudoflow that were noted in areas lacking vascular flow in the overlying retina. Eight eyes exhibited suspended scattering particles in motion. In 26 of 30 eyes with nonneovascular AMD, pseudoflow associated with macular drusen of any type was noted. Two of 11 eyes with small drusen, 16 of 17 eyes with medium or large drusen, 5 of 5 eyes with drusenoid pigment epithelial detachment, 12 of 16 eyes with ribbon-like subretinal drusenoid deposits, and 13 of 17 eyes with dot-like SDD exhibited pseudoflow.

Conclusions: Pseudoflow due to projection artifact is common in eyes with hard exudates or macular drusen. 3D PAR reduces but does not eliminate pseudoflow, and pseudoflow may be detected within the foveal avascular zone, indicating that other factors, such as Z-axis micromotion, may also contribute to pseudoflow.

Translational Relevance: This study provides insight into the etiology of pseudoflow noted on OCTA and will guide more accurate clinical interpretation and investigation of OCTA images.

Introduction

Optical coherence tomography angiography (OCTA) uses the principle of decorrelation, that is differences in the amplitude or phase component of motion between sequential optical coherence tomography (OCT) B-scans obtained at precisely the same

cross-section, to detect motion contrast. Stationary tissue structures exhibit a minimal decorrelation signal, whereas moving structures such as blood flow exhibit a high decorrelation signal, enabling the identification of microvascular flow.

Application of this new technology in the clinical setting requires recognition of artifacts that may confound analysis.^{1,2} Commonly encountered OCTA

artifacts include projection, motion or blinking, masking or unmasking, and segmentation artifacts.^{1,2} Falavarjani et al.³ recently demonstrated that these artifacts are more common in eyes with pathology and failure to correctly interpret these associated findings may lead to incorrect diagnosis or inaccurate conclusions regarding disease pathophysiology. OCTA artifacts resulting in falsely elevated signal intensity can be clearly attributable to a specific type of artifact in certain cases. For example, falsely increased OCTA signals corresponding to true vascular flow can be generated by unmasking due to geographic atrophy (e.g., nonneovascular, or dry, age-related macular degeneration [AMD]), leading to falsely elevated choroidal signals through regions of retinal pigment epithelium (RPE) loss.⁴⁻⁶ In other cases, however, identification of OCTA artifact and the underlying etiology can be more challenging. In eyes with diabetic retinopathy, OCTA can enhance the detection of microaneurysms not identified with fluorescein angiography,⁷ but certain flow signals may represent artifacts attributed to z-axis micro-motion of hard exudates.^{1,8} Additionally, OCTA also has the ability to generate motion contrast associated with nonvascular flow due to Brownian motion of suspended macromolecules in cystic cavities, as recently described by Kashani et al.^{4,9} who have coined the term “suspended scattering particles in motion” (SSPiM).⁷

Perhaps the most common source of false positive blood flow signals identified via OCTA is projection artifact.¹ Analyzing OCT B-scans with flow overlay will show this form of artifact as “projection tails” beneath superficial vessels as decorrelated light encounters highly reflective posterior structures, such as the ellipsoid zone band and RPE/Bruch’s membrane complex.¹ Projection artifact falsely identified as true blood flow can confound analysis of drusen and outer retinal hyperreflective lesions associated with type 3 neovascularization in eyes with AMD.¹⁰⁻¹⁴

Given the prevalence of projection artifact, concerted effort has been devoted to the development of projection artifact removal algorithms. Traditional two-dimensional algorithms rely on image segmentation and a slab subtraction strategy, which require accurate segmentation of retinal layers to isolate the superficial vascular plexus signal that can then be subtracted from the deeper segmentation.¹⁵ These strategies are limited because of the inaccuracy of segmentation in eyes with pathology and because of the loss of true flow information due to signal subtraction. More recently, volume-based

or three-dimensional projection artifact removal algorithms have been developed that bypass the need for accurate segmentation.¹⁶ An example of this algorithm is Optovue’s proprietary 3D PAR system that compares intensity-normalized decorrelation values between three-dimensional voxels across the same axial scan line and removes projection artifact from true flow in both the en face and cross-sectional OCTA planes.

The purpose of this study was to assess the nature and prevalence of false positive OCTA blood flow signals caused by hyperreflective lesions in the macula, such as hard exudates and drusen, and to assess the efficacy of 3D PAR for these artifact cases. OCTA images from patients with diabetic macular edema (DME), retinal vein occlusion (RVO), and nonneovascular AMD were analyzed for false positive blood flow signals detected by en face OCTA imaging and OCTA B-scan overlays to better understand the etiology of these forms of flow artifact.

Methods

This was a retrospective review of OCTA imaging performed on a series patients evaluated at the Stein Eye Institute between the months of January 2015 and December of 2017. Informed consent was obtained from all subjects, and the study was conducted in accordance with the Declaration of Helsinki and Health Insurance Portability and Accountability Act bylaws and was approved by the institutional review board of the University of California Los Angeles.

Inclusion criteria included the presence of hard exudates associated with DME or RVO or the presence of macular drusen associated with nonneovascular AMD or familial drusen based on retinal examination with slit lamp biomicroscopy and confirmed by spectral domain-OCT (SD-OCT). Clinical data collected included age, sex, and Snellen visual acuity (VA). Staging of diabetic retinopathy and differentiation of branch RVO (BRVO) versus central RVO (CRVO) were noted, and history of anti-vascular endothelial growth factor (VEGF) therapy, intravitreal steroid therapy, and laser treatment were all recorded. For eyes with macular drusen, the type of drusen were recorded based on slit lamp biomicroscopy and SD-OCT imaging.

All eyes were imaged with a commercial SD-OCTA device (Optovue AngioVueHD; Optovue Inc, Fremont, CA, USA) by using the split-spectrum

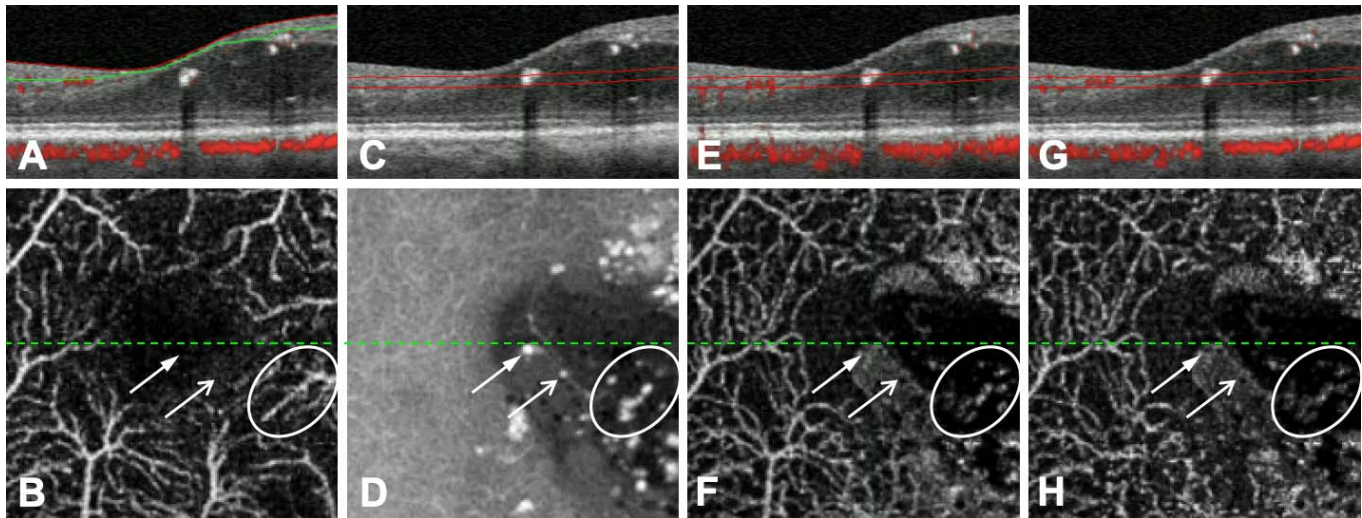


Figure 1. Hard exudates in an eye with DME. Structural OCT with angio overlay (A) with segmentation through the superficial retina demonstrates the foveal avascular zone via en face OCTA (B, image size 1.5×1.5 mm). Structural OCT (C) with thin slab segmentation through focal hard exudates within the foveal avascular zone with corresponding en face structural OCT (D, image size 1.5×1.5 mm). Note two hard exudates within the foveal avascular zone (*arrows*) associated with an area of SSPiM and a group of hard exudates outside of the foveal avascular zone (*oval*). Structural OCTA with angio overlay (E) without 3D PAR with corresponding thin slab segmentation at the level of the hard exudates fails to display corresponding false positive blood flow signal, or pseudoflow, for exudates within the foveal avascular zone (*arrows*), but pseudoflow is identified for hard exudates (*oval*) outside of the foveal avascular zone (F, image size 1.5×1.5 mm). The false positive blood flow signals associated with hard exudates (*oval*) are reduced but not eliminated by activation of 3D PAR (G and H, image size 1.5×1.5 mm).

amplitude decorrelation angiography algorithm. The Optovue system uses an 850-nm center wavelength, at a speed of 70,000 A-scans per second. Each 3×3 -mm² OCTA volume scan contained 304×304 A-scans and each 6×6 -mm² OCTA volume scans contained 400×400 A-scans. Both scan protocols used two consecutive B-scans to perform image decorrelation. Both the 3×3 -mm² and 6×6 -mm² scan protocols were centered on the fovea. All images were analyzed with and without 3D PAR. Unless otherwise stated, all images are presented with 3D PAR software activated (software version 2017.1.0.151). If multiple scans were available for the same eye, the scan with the highest scan quality and highest signal strength index (SSI) were chosen for analysis, as lower scan quality was noted to increase pseudoflow signal (see Fig. 6). Images were excluded if the OCTA SSI was less than 40, if the quality index was less than 5 out of 10, or if other significant artifact was present, specifically motion artifact resulting in gap defects, quilting defects, stretch artifacts, or white line artifacts as defined by Spaide et al.¹

OCTA images were analyzed using a superficial retinal slab to analyze the superficial vascular plexus and thin slab segmentation to study the outer retina and RPE/Bruch's complex. The boundaries of the

superficial retinal slab extended from the internal limiting membrane to the superficial inner plexiform layer. This slab contained the capillary networks feeding the nerve fiber layer, ganglion cell layer, and boundary of the inner nuclear layer and inner plexiform layer. Automated segmentation was manually corrected if registration error was identified. Example superficial retinal slabs are shown in Figures 1B and 2B. Thin segmentation was defined as segmentation aligned to the choriocapillaris with a 40 micron offset. The thin slab was then aligned with the hard exudates or drusen when examining eyes with macular edema or macular degeneration, respectively. This segmentation was selected for assessment of the hard exudates, as it is commonly used to evaluate neovascularization in the outer retina, which is typically avascular and can be prone to contamination by artifact signals. All images were analyzed by the same two authors (K.K.H. and A.A.) on two separate occasions to ensure accuracy of the grading. Discrepancies, if present, were adjudicated by the senior author (D.S.). The term "pseudoflow" was used to describe false positive flow signals, believed to be artifact, detected on either en face OCTA or OCT B-scans with flow overlay in areas of stationary hyperreflective struc-

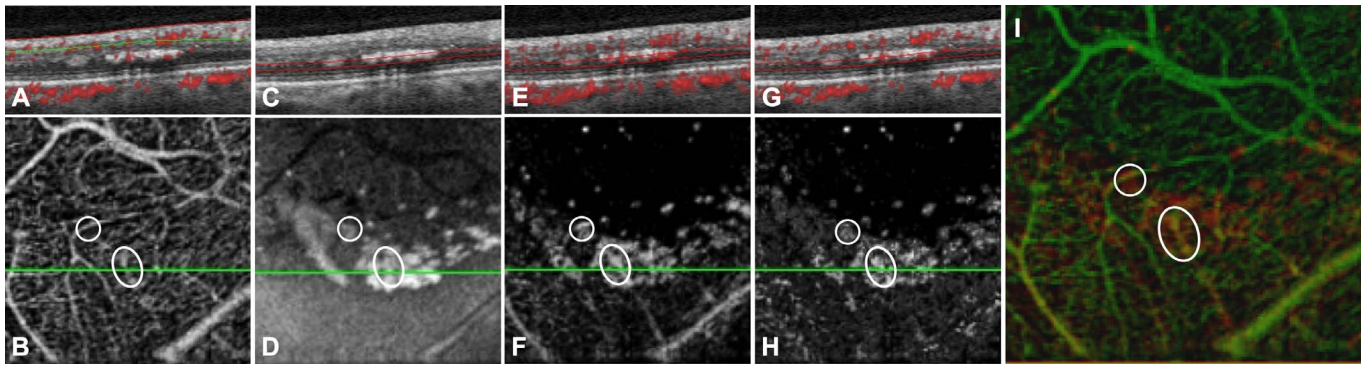


Figure 2. Confluent hard exudates from an eye with DME. OCT B-scan with flow overlay (A) and en face OCTA displays the superficial retinal capillary plexus (B, 1.5×1.5 mm). OCT B-scan (C) and en face structural OCT (D, 1.5×1.5 mm) illustrate the diffuse confluent exudates. Structural OCT B-scan with angio overlay (E) and en face OCTA scan (F, 1.5×1.5 mm) with thin slab segmentation through the confluent hard exudates without 3D PAR demonstrates strong false positive blood flow signals, or pseudoflow, that clearly mirror the overlying vasculature (F). OCT B-scan with flow overlay (G) and en face OCTA scan (H, 1.5×1.5 mm) with thin slab segmentation through the hard exudates with 3D PAR activation demonstrates decreased but not eliminated false positive blood flow signals that continue to mirror the overlying vasculature (B). An overlay (I, 1.5×1.5 mm) of panel B and panel F highlight the projection of the superficial vascular plexus (green) onto the hard exudates (red) with the overlap appearing yellow, as highlighted in the circle and oval outlines.

tures, such as hard exudates and drusen, and judged to be unrelated to true vascular flow or SSPiM at these locations.⁴

Image Analysis of Eyes with Macular Edema

Hard exudates were identified as radial or dot-like hyperreflective foci with near-infrared (NIR) imaging and as hyperreflective outer retinal foci with cross-sectional or en face structural OCT. For the purposes of this study, confluent hard exudates were defined as patches of hard exudates that spanned an area larger than 0.25 mm^2 (approximate area of the foveal avascular zone [FAZ]), as analyzed via en face structural OCT.¹⁷ SSPiM was identified as previously described by Kashani et al.^{4,9} and Matsunaga et al.⁷ Briefly, hyperreflective intraretinal cystic pockets of fluid noted via structural OCT were examined for corresponding coregistered extravascular flow signal via both en face and cross-sectional OCTA. The presence of SSPiM signal was noted if OCTA confirmed a moderately homogeneous flow signal that coregistered with the hyperreflective intraretinal cystic cavity.

Hard exudates were then studied for corresponding false positive blood flow signals by examining the corresponding thin segmentation en face OCTA slab for coregistered signals. Additionally, the cross-sectional OCTA overlay of the OCT B-scan through the hard exudates was also studied to analyze the flow signal. Hyperreflective foci that demonstrated flow origin from the surrounding microvasculature via en

face OCTA were characterized as true microvascular abnormalities and were excluded from the analysis. Analysis of several OCT and OCTA anatomic features of hard exudates, including confluence and size and location of hard exudates (in the FAZ versus in areas of capillary nonperfusion versus in areas of intact overlying vasculature), was performed.

Image Analysis of Eyes with Macular Drusen

Macular drusen and subretinal drusenoid deposits (SDDs) (i.e., reticular pseudodrusen) were identified as hyperreflective deposits under the RPE or between the RPE and outer retina, respectively, by cross-sectional or en face structural OCT. Drusen were categorized as small drusen ($<63 \mu\text{m}$ diameter), medium and large drusen (≥ 63 to $125 \mu\text{m}$ diameter), drusenoid pigment epithelial detachment (PED) (confluent soft drusen > 250 microns), ribbon-like SDD, and dot-like SDD (see Fig. 5).^{18–20} Size of drusen was confirmed by measurement of basal drusen diameter by using the proprietary caliper modality of SD-OCT available in the Optovue software. SDDs were confirmed using NIR imaging.

Drusen and SDD were then examined for corresponding false positive blood flow signal by using thin segmentation at the level of the outer nuclear layer immediately above or abutting the drusen surface. This level of segmentation was chosen because false positive blood flow signals associated with drusen are most prominent when compared with the hyporeflexive, avascular outer nuclear layer. En face OCTA

was first analyzed for pseudoflow corresponding to drusen on the en face structural OCT and confirmed with B-scan OCTA overlay. False positive blood flow signals were analyzed with and without the activation of 3D PAR. If a drusenoid or serous PED was noted, thin slab segmentation through the PED and manual segmentation along the RPE contour of the PED was analyzed to exclude any evidence of neovascularization, as suggested previously.^{12,13}

Results

False Positive Blood Flow Signal Associated with Hard Exudates

Ten eyes from 10 patients (3 male and 7 female) with RVO (4 with CRVO and 6 with BRVO) associated with macular edema and lipid exudates were included. The mean age was 69 ± 14 years with mean VA 20/45 (range, 20/30 to 20/600). Eight of 10 (80%) eyes displayed isolated RVO, whereas 1 eye was complicated by an associated reperfused cilioretinal artery occlusion and a second eye was noted to have an epiretinal membrane and primary open angle glaucoma treated with latanoprost. Nine of 10 (90%) eyes had received treatment for the macular edema and exudates (9 with anti-VEGF therapy, 4 with focal macular laser, and 3 with dexamethasone implant) (Table 1). Ten eyes from 7 patients (3 male and 4 female) with DME and a grading that ranged from moderate nonproliferative diabetic retinopathy (NPDR) to quiescent proliferative diabetic retinopathy were also included in the analysis. The mean age was 60 ± 7 years and mean VA was 20/34 (range, 20/30 to 20/300). None of the eyes displayed any additional diagnoses that could contribute to the development of macular edema. Nine of 10 (90%) eyes had received treatment (9 with anti-VEGF therapy, 5 with focal macular laser, and 3 with dexamethasone implant) (Table 1).

Twenty out of the 20 (100%) eyes exhibited OCTA false positive blood flow signals due to focal lipid exudates that displayed characteristic hyperreflectivity with NIR imaging and cross-sectional and en face structural OCT. False positive blood flow signals were further confirmed by excluding an origin from and connection to the surrounding microvasculature via en face OCTA, as noted in the methodology. False positive blood flow signals were often more prominent with en face OCTA using thin slab segmentation through the focal exudates versus flow overlay of the OCT B-scan. In fact, 5 of 20 (25%) eyes with focal

exudates demonstrating false positive blood flow signals with en face OCTA did not show obvious false positive signals on the flow overlay of the OCT B-scan. When examining OCTA overlay of the OCT B-scan, hard exudates were clearly demonstrated as hyperreflective foci typically located in the outer plexiform layer, inner nuclear layer, or inner plexiform layer with coregistered flow signals noted on the corresponding OCTA overlay over the hard exudate (see Fig. 1). Notably, false positive blood flow signals were brighter if the hard exudate was located directly underneath a true flow signal generated by the superficial vascular plexus suggestive of “decorrelation tail” artifact.^{1,21} In all 20 eyes, false positive blood flow signals corresponding to hard exudates persisted despite the use of the 3D PAR that successfully reduced the intensity of the false positive blood flow signals but did not eliminate them entirely.

Confluent hard exudates were noted in 4 of the 20 (20%) cases and the pattern of the false positive blood flow signal was different versus the focal exudates. Confluent hard exudates displayed a false positive signal pattern that was not homogenous over the entire extent of the exudate (see Fig. 2). The en face OCTA pattern clearly mirrored that of the overlying capillary plexus. Additional OCTA analysis of confluent hard exudates using the OCT B-scan overlay demonstrated that the intensity of the false positive signal clearly mirrored the intensity of the true OCTA flow signal of the overlying superficial capillary plexus. As with the focal false positive signal of single hard exudates, in all 4 eyes with confluent exudates, the mirrored false positive blood flow signal was reduced but not eliminated by projection removal software.

The only factor contributing to the presence or absence of false positive blood flow signal was the presence and perfusion of the overlying retinal capillary plexus, as determined using the superficial retinal slab. Specifically, 7 of 20 (35%) analyzed eyes concurrently exhibited some hard exudates that did not display a false positive signal by either flow overlay or en face OCTA. In all such cases, hard exudates were localized in areas without overlying flow in the overlying capillary plexus, that is adjacent to or in the FAZ or in areas of capillary nonperfusion (see Fig. 1).

Eight of 20 (40%) eyes independently and concurrently demonstrated SSPiM. SSPiM was differentiated from flow artifact associated with hard exudates by the homogeneity of the OCTA signal. Hyperreflective cystic cavities with SSPiM illustrated a relatively

Table 1. Patient Characteristics, Diagnosis, Prior Treatment, and OCTA Findings for Eyes with Macular Edema and Hard Exudates

Patient	Eye	Age (years)	Sex	VA	Diagnosis	Other Causes of Macular Edema	Prior Treatments	SSPiM	Hard Exudates with False Positive Flow	Hard Exudates without False Positive Flow
1	Left	72	F	20/30	CRVO	None	aV, D	Yes	Yes	Yes - FAZ
2	Right	74	M	20/40	CRVO	None	aV	No	Yes	No
3	Left	76	F	20/600	BRVO	None	FML, aV	No	Yes	Yes - capillary nonperfusion
4	Right	33	F	20/70	CRVO	None	None	No	Yes	Yes - capillary nonperfusion
5	Right	75	F	20/100	BRVO	None	FML, aV	No	Yes	No
6	Left	64	F	20/20	BRVO	None	aV	No	Yes	No
7	Left	69	F	20/50	BRVO	None	aV	Yes	Yes	No
8	Right	76	F	20/30	BRVO	None	FML, aV, D	No	Yes	Yes - capillary nonperfusion
9	Right	83	M	20/50	BRVO s/p TRP	ERM, xalatan	FML, aV, D	No	Yes	No
10	Right	72	M	20/80	CRVO	None	aV	No	Yes	No
11	Right	67	F	20/30	mod NPDR	None	aV	Yes	Yes	No
	Left	67	F	20/30	mod NPDR	None	None	Yes	Yes	Yes - FAZ
12	Left	64	M	20/30	mod NPDR	None	aV	Yes	Yes	No
13	Right	62	M	20/25	severe NPDR	None	FML, aV, D	No	Yes	No
	Left	62	M	20/40	severe NPDR	None	FML, aV, D	No	Yes	No
14	Right	49	F	20/30	PDR s/p PRP	None	aV, D	No	Yes	Yes - capillary nonperfusion
15	Right	58	F	20/30	PDR s/p PRP	None	FML, aV	Yes	Yes	No
	Left	58	F	20/50	PDR s/p PRP	None	FML, aV	No	Yes	No
16	Right	74	F	20/300	PDR s/p PRP	ERM	FML, aV	Yes	Yes	Yes - capillary nonperfusion
17	Right	79	M	20/25	PDR s/p PRP	None	aV	Yes	Yes	No

aV, anti-VEGF; D, dexamethasone implant; ERM, epiretinal membrane; F, female; FML, focal macular laser; M, male; PDR, proliferative diabetic retinopathy; PRP, panretinal photocoagulation; TRP, targeted retinal photocoagulation; s/p, status post.

uniform flow signal unaffected by 3D PAR, which corresponded with the entire cystic cavity and did not vary with the overlying vasculature. The appearance of the moderately hyperreflective cystic cavity on structural OCT further differentiated SSPiM from the bright hyperreflective signal associated with hard exudates.

False Positive Blood Flow Signal Associated with Drusen

Thirty eyes of 25 patients (12 male, 13 female) with macular drusen were analyzed. Mean age was 75 ± 13 years with mean VA 20/26 (range, 20/16 to 20/200). A

total of 11 eyes exhibited small drusen, 17 eyes exhibited medium to large drusen, 5 eyes exhibited drusenoid PEDs, 16 eyes exhibited ribbon-like SDDs, and 17 eyes exhibited dot-like SDDs. Neovascularization, geographic atrophy, retinal vascular disease, and other macular abnormalities were excluded in all eyes (Table 2).

Of the 30 eyes examined, 26 (87%) demonstrated false positive blood flow signals with thin segmentation of the outer nuclear layer due to any type of drusen. Of the 11 eyes exhibiting small macular drusen, 2 (18%) were found to have false positive blood flow signals associated with small drusen (Figs.

Table 2. Patient Characteristics, Diagnosis, and OCTA Findings for 30 Eyes with Drusen

Patient	Eye	Age (years)	Sex	VA	Disease	Drusen Type (+/- Pseudoflow)				
						Small Drusen	Large Drusen	Drusenoid PED	Ribbon-like SDD	Dot-Like SDD
18	Right	67	F	20/20	Dry AMD	Yes (+)	Yes (+)			
19	Left	84	M	20/20	Dry AMD				Yes (+)	Yes (+)
20	Right	64	M	20/40	Dry AMD	Yes (-)	Yes (+)			
21	Right	70	F	20/25	Dry AMD				Yes (+)	Yes (+)
	Left	70	F	20/20	Dry AMD				Yes (+)	Yes (+)
22	Right	36	F	20/20	Familial drusen	Yes (-)	Yes (-)			
	Left	36	F	20/20	Familial drusen	Yes (-)	Yes (+)			
23	Right	79	F	20/20	Dry AMD		Yes (+)		Yes (+)	Yes (+)
	Left	79	F	20/40	Dry AMD		Yes (+)		Yes (+)	Yes (+)
24	Left	67	M	20/20	Dry AMD	Yes (-)	Yes (+)	Yes (+)		
25	Right	74	F	20/30	Dry AMD	Yes (-)	Yes (+)	Yes (+)		
26	Right	67	F	20/20	Dry AMD	Yes (-)	Yes (+)			
27	Right	77	M	20/16	Dry AMD				Yes (+)	Yes (+)
28	Right	76	M	20/60	Dry AMD					Yes (-)
29	Right	94	M	20/25	Dry AMD				Yes (+)	Yes (+)
30	Right	87	M	20/30	Dry AMD				Yes (+)	Yes (+)
31	Right	89	M	20/30	Dry AMD				Yes (-)	Yes (-)
32	Right	60	F	20/25	Dry AMD		Yes (+)		Yes (-)	
	Left	60	F	20/25	Dry AMD		Yes (+)		Yes (+)	
33	Right	83	M	20/25	Dry AMD		Yes (+)	Yes (+)		
34	Left	92	F	20/25	Dry AMD	Yes (+)	Yes (+)			
35	Left	87	F	20/40	Dry AMD				Yes (-)	Yes (-)
36	Right	78	F	20/25	Dry AMD	Yes (-)	Yes (+)			
37	Right	84	M	20/30	Dry AMD	Yes (-)	Yes (+)			
38	Right	86	F	20/60	Dry AMD	Yes (-)	Yes (+)	Yes (+)	Yes (-)	Yes (-)
39	Left	70	M	20/20	Dry AMD					Yes (+)
40	Right	84	F	20/25	Dry AMD		Yes (+)			Yes (+)
41	Right	66	F	20/100	Dry AMD				Yes (+)	Yes (+)
	Left	66	F	20/200	Dry AMD				Yes (+)	Yes (+)
42	Right	89	M	20/16	Dry AMD			Yes (+)	Yes (+)	Yes (+)

AMD, age-related macular degeneration.

3A–D). Of the 17 eyes with medium to large macular drusen, 16 (94%) demonstrated false positive blood flow signals corresponding to the medium to large drusen. False positive blood flow signal strength was correlated with strength of the true flow signal in the overlying vessels as demonstrated by B-scan OCTA overlay (Figs. 3E–H). These signals were reduced but not eliminated by 3D PAR. Of the 5 eyes demonstrating large macular drusen, all were found to have corresponding false positive blood flow signals (Figs. 3I–L). Drusenoid PEDs were notable for clearly

mirroring overlying vasculature on OCTA when analyzed without 3D PAR via en face OCTA and OCTA B-scan overlay. These false positive blood flow signals were dramatically reduced, but not eliminated, with 3D PAR activated (Fig. 3L). Ribbon-like SDDs were noted in 16 eyes, of which 12 (75%) demonstrated false positive blood flow signals, which were reduced with 3D PAR activation (Figs. 3M–P). Dot-like SDDs were found in 17 eyes. False positive blood flow signals associated with dot-like SDDs were found in 13 (76%) eyes (Figs. 3Q–T). Focal false

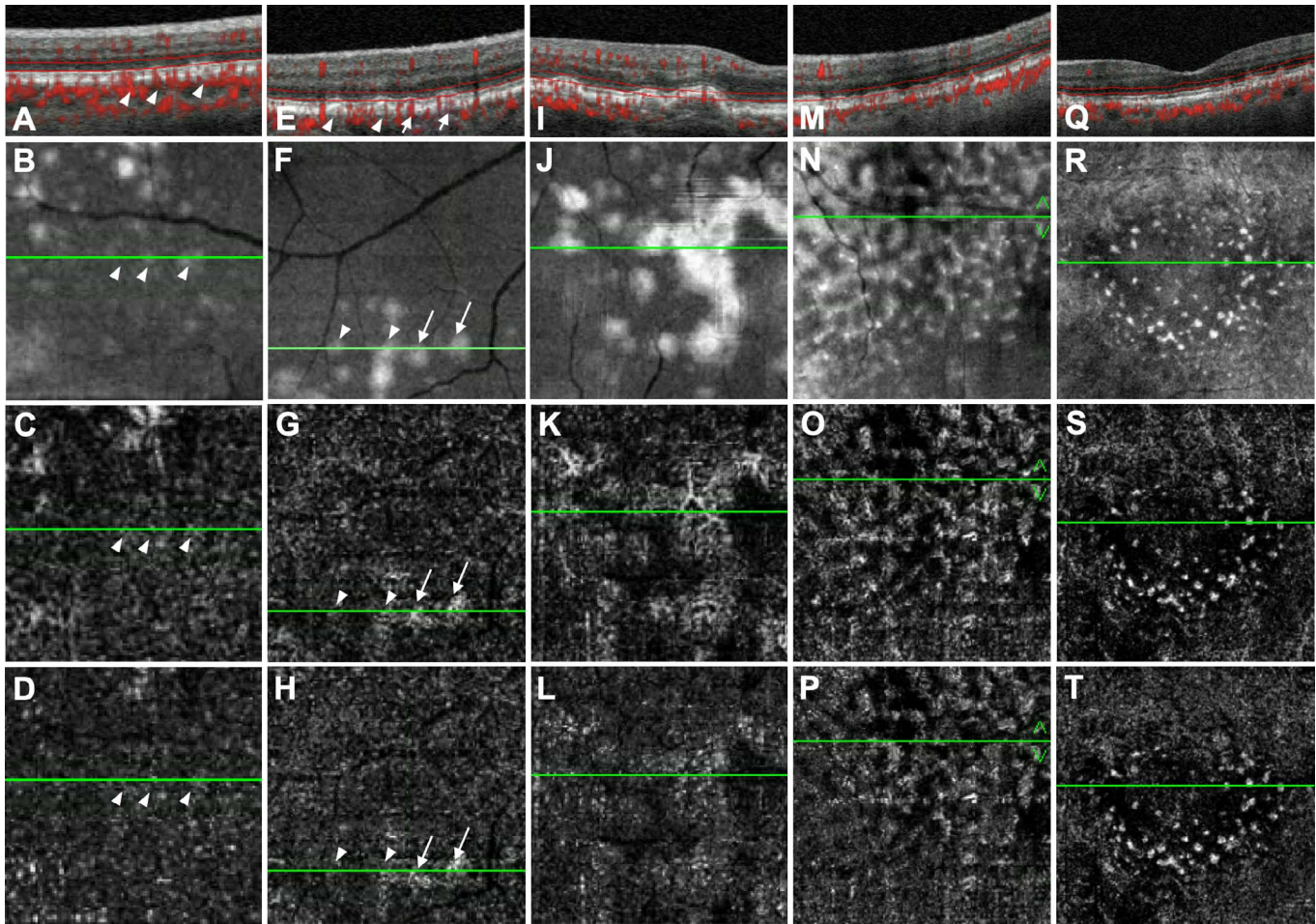


Figure 3. Small macular drusen (*arrowheads*) that are noted with B-scan OCT with angio overlay (A) and with en face structural OCT (B, image size 2×2 mm) do not illustrate a false positive blood flow signal via en face OCTA without 3D PAR (C, image size 2×2 mm) and with 3D PAR (D, image size 2×2 mm) despite significant overlying superficial signal on angio overlay of SD-OCT B-scan overlay (A) due to minimal extension into the outer nuclear layer. Larger macular drusen identified with angio overlay of B-scan OCT (E) and with en face structural OCT (F, image size 2×2 mm) illustrate false positive blood flow signals, that is pseudoflow, corresponding to two drusen with stronger overlying flow in the superficial capillary plexus (*arrows*) and minimal pseudoflow for two drusen with a weak overlying flow signal (*arrowheads*). These false positive blood flow signals are confirmed by en face OCTA without 3D PAR (G, image size 2×2 mm) and with 3D PAR (H, image size 2×2 mm). Large drusenoid PED identified with angio overlay of B-scan OCT (I) and en face OCT (J, image size 2×2 mm) display clear projection of overlying vessels via en face OCTA without 3D PAR (K, image size 2×2 mm), which is reduced but not eliminated with activation of 3D PAR (L, image size 2×2 mm). Ribbon-like SDDs identified with angio overlay of B-scan OCT (M) and with en face structural OCT (N, image size 3×3 mm) demonstrate corresponding false positive blood flow signals, or pseudoflow, with en face OCTA without 3D PAR (O, image size 3×3 mm) and with 3D PAR (P, image size 3×3 mm). Dot-like SDDs identified with angio overlay of B-scan OCT (Q) and with en face structural OCT (R, image size 3.5×3.5 mm) illustrate corresponding pseudoflow with en face OCTA without 3D PAR (S, image size 3.5×3.5 mm) and with 3D PAR (T, image size 3.5×3.5 mm).

positive blood flow signals associated with drusen of all types were noted to increase with decreased scan quality. This finding was noted in 14 out of 14 eyes, which had multiple scans for comparison.

Eight of the 30 eyes also illustrated medium-to-large soft macular drusen or drusenoid PEDs in the FAZ. One of these 8 cases demonstrated false positive blood flow signals overlying a drusenoid PED, which straddled the border of the FAZ. The false positive

blood flow signal was not limited to the RPE elevation outside the FAZ but was also generated by the segment of RPE elevation within the FAZ, indicating that projection artifact was not the only etiology for the false positive OCTA signal. OCTA with thin slab segmentation contoured to the RPE and underneath the RPE elevation through the drusenoid PED did not illustrate any flow signal, excluding neovascularization.

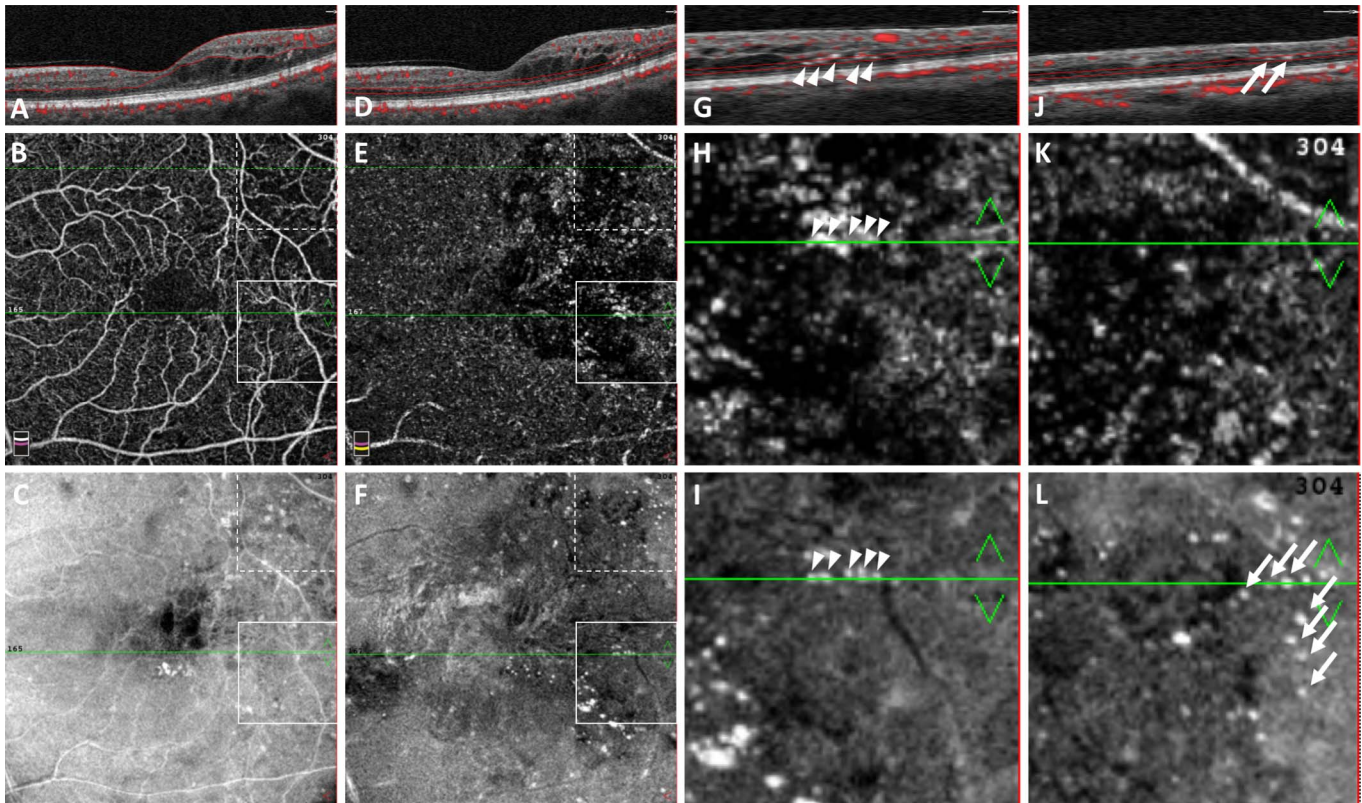


Figure 4. Case 1. A 72-year-old female with history of glaucoma referred for CRVO and cystoid macular edema (CME) of the left eye. OCT B-scan (A) with flow overlay illustrates CME and outer retinal hyper-reflective foci and the level of segmentation for B and C. En face OCTA (B, image size 6×6 mm) and en face OCT (C, image size 6×6 mm) of the inner retina illustrate superotemporal capillary nonperfusion (*dotted box*), whereas capillaries are perfused within *solid box*. OCT B-scan with flow overlay (D) shows the segmentation for E and F. En face OCTA (E, image size 6×6 mm) and en face OCT (F, image size 6×6 mm) with thin slab segmentation of the outer retina illustrate the presence of cystic cavities and hard exudates. More detailed high magnification analysis (G–I) of an area with intact overlying vasculature denoted by *solid white box* with thin slab segmentation of the outer retina illustrates hard exudates via B-scan and en face OCT (G and I, *arrowheads*) with corresponding false positive blood flow signals, or pseudoflow, via en face OCTA (H, *arrowheads*). More detailed high-magnification analysis of inset of an area of capillary nonperfusion (J–L), denoted by *dotted white box* with thin slab segmentation of the outer retina, shows hard exudates via B-scan and en face structural OCT (J and L, *arrows*) without any evidence of pseudoflow (K). Images presented with 3D PAR activated.

Case 1

A 72-year-old female with glaucoma (not treated with a prostaglandin analog) and diabetes (without retinopathy) was referred for evaluation of CRVO and treatment of macular edema of the left eye. Visual acuity was 20/20 in the right eye with funduscopic examination notable only for optic disc cupping. Visual acuity was 20/30 in the left eye after previous intravitreal bevacizumab and ranibizumab injections and a dexamethasone implant. Funduscopic examination of the left eye was notable for mild optic disc cupping, vessel tortuosity, and macular edema due to CRVO. Multimodal imaging of the left eye included SD-OCT, which illustrated cystoid macular edema and scattered hard exudates. En face OCTA of the left

eye displayed a superotemporal area of flow deficit or capillary nonperfusion (Fig. 4B). Hard exudates with corresponding false positive blood flow signals, that is pseudoflow, were noted underlying areas of intact microvasculature (Figs. 4H, 4I). Additionally, hard exudates without corresponding false positive blood flow signals were noted underlying the demarcated area of capillary nonperfusion (Figs. 4K, 4L).

Case 2

A 65-year-old diabetic female was referred for treatment of DME. Visual acuity was 20/30 in both eyes without previous treatment. Retinal examination displayed scattered microaneurysms and dot-blot hemorrhages in both eyes, consistent with moderate NPDR. Circinate exudates and foveal involving

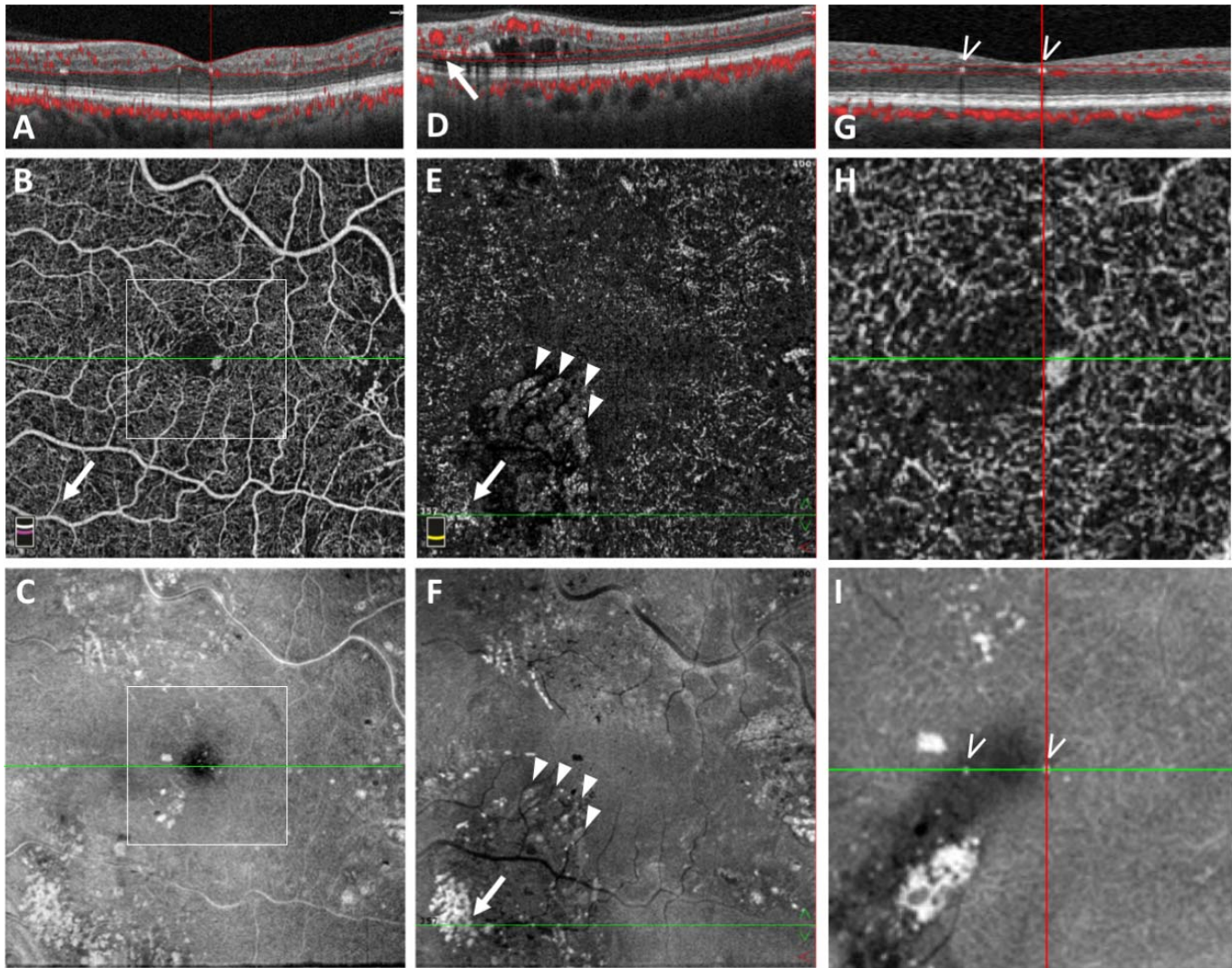


Figure 5. Case 2. A 65-year-old female with untreated NPDR and macular edema of the left eye. OCT B-scan with flow overlay (A) illustrates scattered hard exudates and segmentation for B and C. En face OCTA of the inner retina (B, image size 6×6 mm) demonstrates a central parafoveal microaneurysm and temporal area of capillary flow deficit (i.e., ischemia). Corresponding en face OCT (C, image size 6×6 mm) displays scattered hard exudates and an area of confluent hard exudates in the inferonasal macula. En face OCTA of the same patient with thin slab segmentation of the outer retina (E, image size 6×6 mm) demonstrates SSPiM (arrowheads) which corresponds with hyperreflective fluid-filled cystic pockets identified with en face SD-OCT (F, arrowheads, image size 6×6 mm). Segmentation of the outer retina also illustrates a false positive blood flow signal (E, arrow), or pseudoflow, originating from confluent hard exudates in the inferonasal macula, which reflects the overlying microvasculature noted with the en face OCTA segmentation of the inner retina (B, arrow). OCT B-scan with flow overlay (D) illustrates obvious pseudoflow corresponding to the hard exudates (D, arrow) with overlying true flow signal. Higher magnification view of the foveal avascular zone (imaging area outlined with white box in B and C) displays two hard exudates by both SD-OCT B-scan (G, hollow arrow) and en face SD-OCT (I, hollow arrow), which do not exhibit corresponding false positive blood flow signals by en face OCTA (H) or flow overlay of OCT B-scan (G) due to location in the FAZ. Images presented with 3D PAR activated.

macular edema was noted in the left eye. Multimodal imaging of the left eye including SD-OCT (Fig. 5C) illustrated cystoid macular edema, scattered hard exudates with an area of confluent hard exudates in the inferonasal macula, and hyperreflective cystic cavities. OCTA of the left eye with segmentation of

the inner retina clearly demonstrated a perifoveal microaneurysm and temporal macular capillary ischemia with flow deficit (Fig 5B). En face OCTA of the left eye with thin segmentation of the outer retina illustrated SSPiM signal in the inferonasal macula colocalizing with the hyperreflective cystic cavities

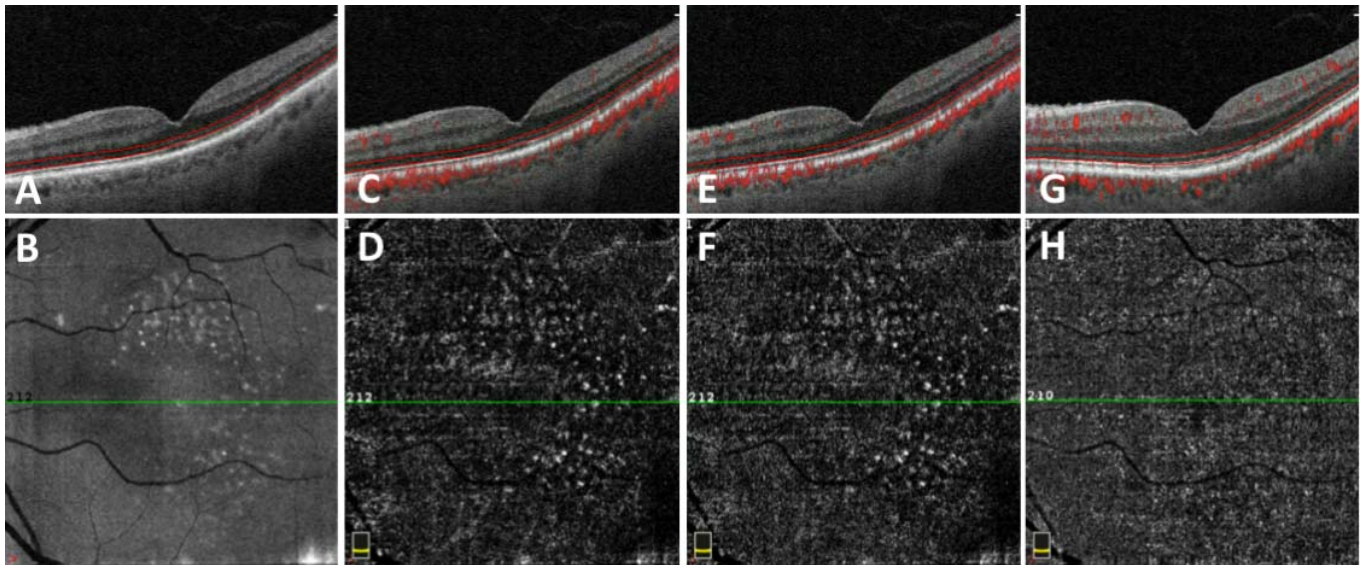


Figure 6. Case 3. A 70-year-old female with macular degeneration and dot-like SDDs of the left eye. Structural OCT B-scan (A) with corresponding en face OCT (B, image size 6×6 mm) illustrate dot-like SDDs. OCTA B-scan angio overlay (C) and en face OCTA (D, image size 6×6 mm) without 3D PAR activation display false positive blood flow signals, or pseudoflow, corresponding to the dot-like SDDs, although the pseudoflow is more readily appreciated with the en face OCTA (image size 6×6 mm) due to dynamic range. These false positive blood flow signals are reduced but not eliminated by activation of 3D PAR (E and F). Angio overlay of OCT B-scan and en face OCTA (image size 6×6 mm) at the same segmentation with improved scan quality illustrates significantly decreased false positive blood flow signals corresponding to the dot-like SDDs (G and H). The origin of the pseudoflow may be explained by projection artifact from the intact overlying vascular plexus reflected off the drusen or z-axis micromotion.

(Figs. 4E, 4F, arrowheads) and false positive blood flow signals, or pseudoflow, generated by an area of confluent hard exudates due to projection from the overlying microvasculature despite the activation of projection artifact removal software (Figs. 5B, 5E, arrow). Detailed analysis of two hard exudates in the FAZ (Figs. 5G, 5I, hollow arrow) was performed, and these two exudates failed to exhibit corresponding false positive blood flow signal by either flow overlay of the OCT B-scan (Fig. 5G) or with the en face OCTA (Fig. 5H) scan.

Case 3

An 80-year-old female was referred for evaluation of macular drusen. Visual acuity was 20/20 in the left eye with retinal examination demonstrating dot-like reticular pseudodrusen. Multimodal imaging of the left eye including SD-OCT illustrated SDDs (Figs. 6A, 6B). OCTA (scan quality 6/10) without 3D PAR with thin slab segmentation at the level of the subretinal hyperreflective drusenoid deposits displayed false positive blood flow signals (Figs. 6C, 6D) or pseudoflow, which was minimally reduced with 3D PAR activation (Figs. 6E, 6F). The false positive blood flow signal was reduced on a subse-

quent scan with improved scan quality (scan quality 8/10) at the same segmentation (Figs. 6G, 6H). There was no evidence of neovascularization to explain the OCTA signal associated with the macular pseudodrusen in the left eye.

Case 4

A 76-year-old male was referred for evaluation of AMD. Visual acuity in the right eye was 20/20 with a history of treated neovascular AMD. Retinal examination of the right eye was notable for pigmentary alterations and drusen. Vision in the left eye was 20/20. Retinal examination of the left eye demonstrated macular drusen. Multimodal imaging of the left eye, including SD-OCT, illustrated confluent macular drusen with a subfoveal drusenoid PED (Figs. 7D, 7F). With thin segmentation at the level of the drusen apices through the outer nuclear layer, OCTA displayed a false positive blood flow signal with both the en face and cross-sectional angio OCT overlay B-scan (Fig. 7E). OCTA segmentation contoured to the RPE and through the middle of the PED failed to exhibit any evidence of a true OCTA flow signal, consistent with choroidal neovascularization (Fig. 7H). Notably, the portion of

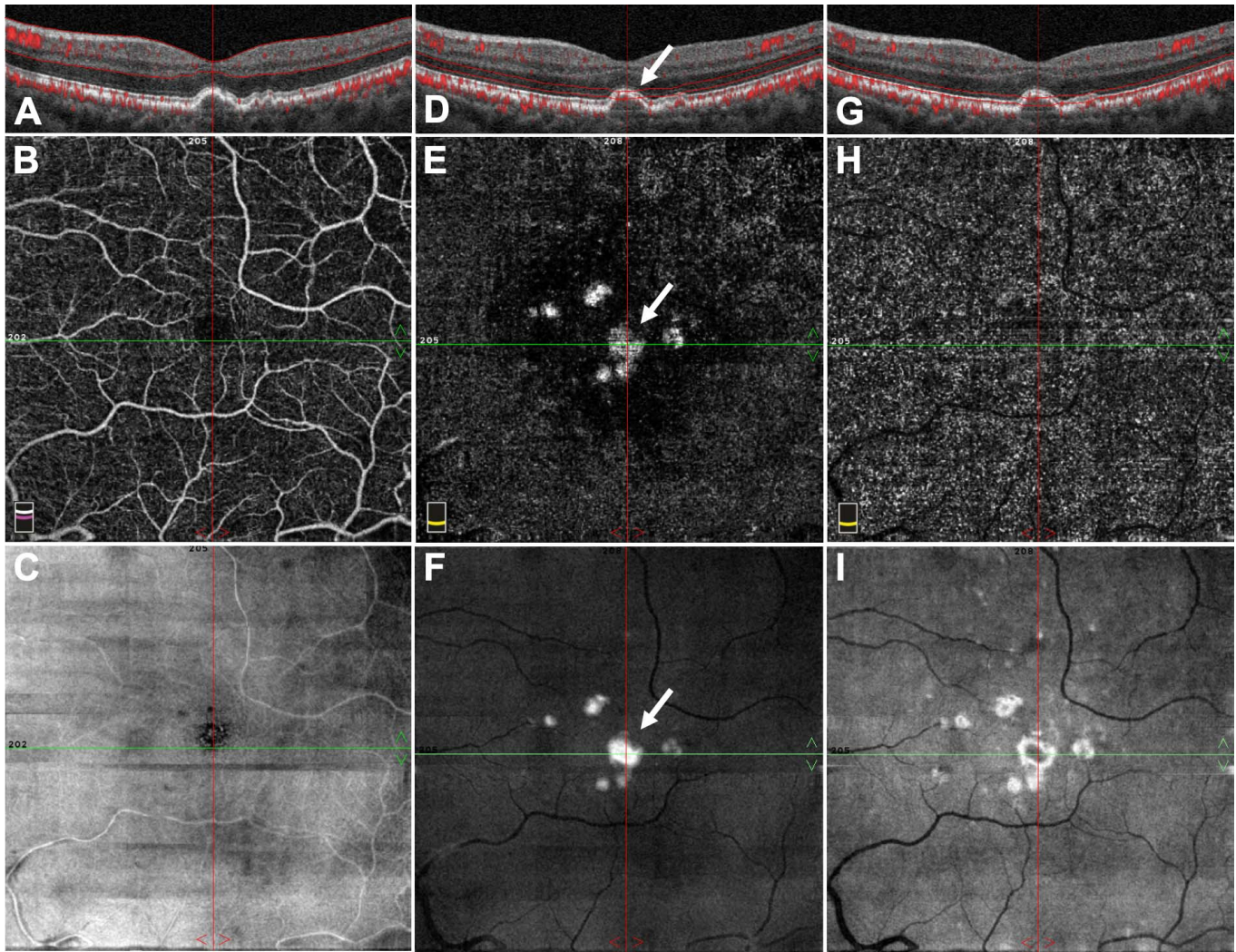


Figure 7. Case 4. A 76-year-old male with nonneovascular AMD of the left eye with confluent soft drusen and subfoveal drusenoid pigment epithelial detachment. B-scan OCT with flow overlay (A) illustrates segmentation through the superficial retinal capillary plexus. With en face OCTA (B, image size 6×6 mm) and en face structural OCT (C), the superficial retinal capillary plexus is identified and is unremarkable. Cross-section B-scan OCT (D) and en face OCTA (E, image size 6×6 mm) and en face structural OCT (F, image size 6×6 mm) thin slab segmentation through the outer retina illustrate false positive blood flow signals, or pseudoflow, which colocalize with hyperreflective macular drusen identified with en face OCT (F, image size 6×6 mm). Notably the drusenoid pigment epithelial detachment straddles the inferior border of the FAZ and illustrates false positive blood flow signals that extend into the foveal avascular zone (D–F, arrow). OCTA generated with thin slab segmentation through the drusenoid pigment epithelial detachment below the RPE elevation (G) fails to display a true OCTA flow signal (H, image size 6×6 mm) of neovascularization. Pseudoflow in the FAZ may represent z-axial micromotion artifact or an alternative artifact mechanism other than projection. Images presented with 3D PAR activated.

the PED outside of the FAZ exhibited a stronger false positive blood flow signal than the portion of the PED within the FAZ.

Discussion

OCTA has enhanced the diagnosis and analysis of microvascular abnormalities associated with retinal

vascular disease and AMD, with clear advantages over dye angiography.^{14,22–24} However, OCTA evaluation can be confounded by various forms of artifact. Notably, pathological lesions with hyperreflective surfaces, such as hard exudates and drusen, can also display false positive blood flow or pseudoflow, as exhibited in this study. Characterization of these findings provide insight into the generation of

these imaging artifacts and allow increased accuracy in the interpretation of OCTA in the clinical setting.^{1,3}

In our study, hard exudates exhibited false positive blood flow signals that varied in breadth according to the confluent area of the exudates and varied in signal intensity according to the flow in the overlying vasculature despite the activation of projection resolution. Additionally, we noted that structures that were more hyperreflective had the highest propensity to produce pseudoflow signals. The lack of a false positive blood flow signal from hard exudates that were located under regions of capillary flow deficit or nonperfusion (i.e., ischemia) further supported the conclusion that this false positive signal was the result of projection artifact. In our analysis with thin slab segmentation through the outer retina, the false positive blood flow signal associated with hard exudates was more prominent when demonstrated with en face OCTA than with angio overlay of the structural OCT. We believe that this is related to dynamic range intensity normalization and presentation of data in a 256 grayscale. Specifically, the window of signal intensity for the angio overlay of the structural OCT B-scan includes the brightest OCTA signal of the superficial plexus, and therefore, low-intensity signals (such as false positive signals from hard exudates) are assigned a relatively low value after normalization and conversion to the 256 grayscale.

Although findings of projection artifact associated with drusen have been described by Zheng et al.,^{12,13} our study is the first to note the correlation with drusen type and size and with proximity to the overlying retinal vasculature. We suspect that the closer the lesion is located to the overlying retinal vascular plexus, the more likely the lesion will exhibit false positive blood flow and, hence, the correlation with larger drusen noted in this study. Of note, ribbon-like SDDs are typically low lying, yet exhibited a relatively high rate of false positive blood flow signals (75%). This may be explained by the location of ribbon-like SDDs in the eccentric macula where the outer nuclear layer is thinner, bringing ribbon-like SDDs into closer proximity to the overlying vasculature and by the relatively wider diameter of these deposits, which exposes a larger hyperreflective surface for projection.²⁵ Interestingly, our case series of macular drusen included one case notable for the presence of false positive blood flow signal elicited from a PED that was partially located in the FAZ. Neovascularization was excluded in this case. Careful examination of the false positive blood flow signal indicated that the portion

of the PED in the FAZ displayed a slightly lower signal intensity than the portion of the PED outside of the FAZ. False positive flow signal generated by the drusenoid PED found within the FAZ may be explained by a decorrelated signal caused by micromotion in the z axis. Z-axial micromotion may be due to breathing or pulsation with the cardiac cycle as described by Spaide et al.¹

To our knowledge, this study is the first to characterize in detail pseudoflow artifact associated with hard exudates in macular edema due to diabetic retinopathy and RVO. This retrospective study has provided evidence to suggest that projection artifact is likely the causative process generating these false positive blood flow signals. However, false positive blood flow signals associated with hard exudates are incompletely eliminated by projection removal software, suggesting that current projection removal algorithms (e.g., Optovue 3D PAR) cannot yet be relied on to entirely remove all projection artifact and that other sources of artifact such as z-axial micromotion must be considered. Accurate interpretation of OCTA scans in the study of these diseases must be performed with these limitations in mind to avoid the incorrect interpretation of flow anomalies when none exist. Such analysis may be important in two clinical instances. First, when planning for focal macular laser in eyes with macular edema, it is important to treat true microaneurysms and not hard exudates exhibiting pseudoflow. Second, one must be careful not to confuse vascularized drusen with flow artifact or pseudoflow when determining if anti-VEGF therapy may be indicated. The utility of thin slab segmentation with careful placement of the slab at the apex of the drusen or the PED as compared to slab segmentation through the drusen or PED may help to distinguish pseudoflow from true choroidal neovascularization.

The study has several limitations including the retrospective design, the relatively small sample size, and the nonconsecutive selection of cases, which can introduce ascertainment bias. In addition, only one proprietary device was used in this study. Although this strengthens the consistency of our analysis, it fails to confirm our results across other systems that may be used in clinical practices worldwide. Furthermore, the impact of projection removal algorithms on pseudoflow artifact is limited to an analysis of the role of 3D PAR, a proprietary algorithm limited to Optovue devices. Although all images included in this study were obtained from one device, we suspect that similar artifacts will also be

present in images obtained from other devices, given the universality of projection artifact in OCTA,¹ but this awaits validation. Finally, it should be stated that although this study noted a greater rate of false positive blood flow associated with larger drusen, a truly accurate rate of identification of pseudoflow and measured correlation of drusen height and proximity to the overlying vasculature was not possible due to quantitative limitations in eyes that harbored large numbers of drusen. Future use of specialized image analysis algorithms may provide new avenues toward performing a more quantitative analysis of false positive blood flow signals associated with macular drusen and confluent hard exudates.

In summary, this study demonstrated the importance of recognizing a false positive blood flow signal, or pseudoflow, on OCTA imaging generated by hyperreflective entities deep to the overlying retinal microvasculature. This is particularly important in the analysis of OCTA imaging in patients with retinal vascular disease and AMD where pathologic hyperreflective surfaces associated with macular exudates and macular drusen are commonly identified. Although projection artifact is the likely source of these false positive blood flow signals, micromotion artifact may be an additional factor. It remains to be determined whether additional sources of artifact can also generate pseudoflow associated with hyperreflective lesions.

Acknowledgments

Research was supported by Research to Prevent Blindness Inc, New York, NY (DS) and Macula Foundation Inc, New York, NY (KBF, DS).

Presented in part at the annual meeting of the Association for Research in Vision and Ophthalmology (ARVO), Honolulu, Hawaii, United States, April 29 to May 3, 2018.

Disclosure: **K.K. Hou**, None; **A. Au**, None; **A.H. Kashani**, Carl Zeiss Meditec (F); **K.B. Freund**, Genentech (C, F), Heidelberg Engineering (C), Optovue (C), Novartis (C) Allergan (C), Carl Zeiss Meditec (C); **S.R. Sadda**, Allergan (C, F), Optos (C, F), Genentech (C, F), Iconic (C), Novartis (C), Optovue (C, F), Regeneron (F), Thrombogenics (C), Carl Zeiss Meditec (F); **D. Sarraf**, Amgen (C,F), Bayer (C, F), Genentech (C, F), Heidelberg (F), Novartis (C, F), Optovue (C, F), Regeneron (F), Topcon (F)

References

1. Spaide RF, Fujimoto JG, Waheed NK. Image artifacts in optical coherence tomography angiography. *Retina*. 2015;35:2163–2180.
2. Chen FK, Viljoen RD, Bukowska DM. Classification of image artefacts in optical coherence tomography angiography of the choroid in macular diseases. *Clin Experiment Ophthalmol*. 2016;44:388–399.
3. Falavarjani KG, Al-Sheikh M, Akil H, Sadda SR. Image artefacts in swept-source optical coherence tomography angiography. *Br J Ophthalmol*. 2017;101:564–568.
4. Kashani AH, Green KM, Kwon J, et al. Suspended scattering particles in motion: a novel feature of OCT angiography in exudative maculopathies. *Ophthalmol Retina*. 2018;2:694–702.
5. Waheed NK, Moulton EM, Fujimoto JG, Rosenfeld PJ. Optical coherence tomography angiography of dry age-related macular degeneration. *Dev Ophthalmol*. 2016;56:91–100.
6. Choi W, Moulton EM, Waheed NK, et al. Ultrahigh-speed, swept-source optical coherence tomography angiography in nonexudative age-related macular degeneration with geographic atrophy. *Ophthalmology*. 2015;122:2532–2544.
7. Matsunaga DR, Yi JJ, Koo LOD, Ameri H, Puliafito CA, Kashani AH. Optical coherence tomography angiography of diabetic retinopathy in human subjects. *Ophthalmic Surg Lasers Imaging Retina*. 2015;46:796–805.
8. Coscas G, Lupidi M, Coscas F. Image analysis of optical coherence tomography angiography. *Dev Ophthalmol*. 2016;56:30–36.
9. Kashani AH, Lee SY, Moshfeghi A, Durbin MK, Puliafito CA. Optical coherence tomography angiography of retinal venous occlusion. *Retina*. 2015;35:2323–2331.
10. Bhavsar KV, Jia Y, Wang J, et al. Projection-resolved optical coherence tomography angiography exhibiting early flow prior to clinically observed retinal angiomatous proliferation. *Am J Ophthalmol Case Rep*. 2017;8:53–57.
11. Lumbroso B, Huang D, Chen CJ, et al. *Clinical OCT Angiography Atlas*. New Delhi: JP Medical Ltd; 2015:189.
12. Zhang Q, Zhang A, Lee CS, et al. Projection artifact removal improves visualization and quantitation of macular neovascularization imaged by optical coherence tomography angiography. *Ophthalmol Retina*. 2017;1:124–136.

13. Zheng F, Roisman L, Schaal KB, et al. Artfactual flow signals within drusen detected by OCT angiography. *Ophthalmic Surg Lasers Imaging Retina*. 2016;47:517–522.
14. Kuehlewein L, Dansingani KK, de Carlo TE, et al. Optical coherence tomography angiography of type 3 neovascularization secondary to age-related macular degeneration. *Retina*. 2015;35:2229–2235.
15. Zhang A, Zhang Q, Wang RK. Minimizing projection artifacts for accurate presentation of choroidal neovascularization in OCT microangiography. *Biomed Opt Express*. 2015;6:4130–4143.
16. Zhang M, Hwang TS, Campbell JP, et al. Projection-resolved optical coherence tomographic angiography. *Biomed Opt Express*. 2016;7:816–828.
17. John D, Kuriakose T, Devasahayam S, Braganza A. Dimensions of the foveal avascular zone using the Heidelberg retinal angiogram-2 in normal eyes. *Indian J Ophthalmol*. 2011;59:9–11.
18. Rabiolo A, Sacconi R, Cicinelli MV, Querques L, Bandello F, Querques G. Spotlight on reticular pseudodrusen. *Clin Ophthalmol*. 2017;11:1707–1718.
19. Spaide RF, Curcio CA. Drusen characterization with multimodal imaging. *Retina*. 2010;30:1441–1454.
20. Roquet W, Roudot-Thoraval F, Coscas G, Soubrane G. Clinical features of drusenoid pigment epithelial detachment in age related macular degeneration. *Br J Ophthalmol*. 2004;88:638–642.
21. Louzada RN, de Carlo TE, Adhi M, et al. Optical coherence tomography angiography artifacts in retinal pigment epithelial detachment. *Can J Ophthalmol*. 2017;52:419–424.
22. Inoue M, Jung JJ, Balaratnasingam C, et al. A comparison between optical coherence tomography angiography and fluorescein angiography for the imaging of type 1 neovascularization. *Invest Ophthalmol Vis Sci*. 2016;57:OCT314–OCT323.
23. Nagiel A, Sadda SR, Sarraf D. A promising future for optical coherence tomography angiography. *JAMA Ophthalmol*. 2015;133:629–630.
24. Phasukkijwatana N, Tan ACS, Chen X, Freund KB, Sarraf D. Optical coherence tomography angiography of type 3 neovascularisation in age-related macular degeneration after antiangiogenic therapy. *Br J Ophthalmol*. 2017;101:597–602.
25. Lujan BJ, Roorda A, Croskrey JA, et al. Directional optical coherence tomography provides accurate outer nuclear layer and Henle fiber layer measurements. *Retina*. 2015;35:1511–1520.